Electronic Journal of Structural Engineering

Original Article

Cite this: DOI:10.56748/ejse.24513

Received Date:31 August 2023
Accepted Date:03 March 2024

1443-9255
https://ejsei.com/ejse

Mechanical properties and energy evolution characteristics of karst limestone with different degree of dissolution under uniaxial compression

Jiaqi Guo[ab], Jiheng Gu[a], Erbo Wang[ab], Jianxun Chen[b]*, Qingsong Wang[c]
[a] School of Civil Engineering, Henan Polytechnic University, Jiaozuo, Henan 454003, China
[b] School of Highway, Chang'an University, Xi'an, Shaanxi 710064, China
[c] China Railway 20th Bureau Group Co., Ltd, Xian, Shanxi 710016, China
*Corresponding author: chenjx1969@chd.edu.cn

Abstract

Under the action of dissolution, rock masses form solution fissure leading to changes in their internal structure, which in turn affect their engineering mechanical properties and failure characteristics. Karst rock masses usually have a significant impact on the stability of tunnel surrounding rocks in karst stratum. This article utilizes digital image processing technology and particle flow discrete element method to numerically reconstruct calculation models of limestone with different degree of dissolution. A series of uniaxial compression discrete element numerical experiments were conducted on karst limestone with different degree of dissolution, analyzing the stress-strain relationship, mechanical parameters, failure modes, and energy changes of limestone with different degree of dissolution. Research results indicated the following: (1) The karst limestone model constructed based on digital image processing technology can effectively characterize the dissolution features of karst limestone, and numerical simulation experiments can effectively characterize the mechanical behavior of karst limestone. (2) As the degree of dissolution increases, the stress-strain curve of karst limestone gradually exhibits bimodal or multimodal characteristics, and the uniaxial compressive strength of karst limestone shows an exponential decrease trend, while the elastic modulus shows a linear decrease trend. (3) Under high degree of dissolution, the existence of pore structure causes the stress skeleton inside the karst limestone to be damaged, and the number of shear and tensile cracks is continuously decreasing. The distribution of internal force chains is dispersed, making the karst limestone more prone to failure. (4) During the process of karst limestone failure, most of the input total strain energy is first converted into elastic strain energy, and only a small portion is converted into dissipative strain energy. The increase in the degree of dissolution significantly reduces the total energy input and the storage limit of elastic strain energy during the uniaxial compression failure process of karst limestone and increases the degree of strain energy dissipation.

Keywords

Karst limestone with different degree of dissolution, Mechanical properties, Energy evolution, failure characteristics, Particle flow, Digital image

1. Introduction

China is one of the countries with the widest distribution of karst in the world, with a karst rock distribution area of about 3440000km2, accounting for approximately 35.8% of the land area, especially in Hubei, Chongqing, Sichuan, Yunnan, Guizhou, and other places where karst is densely distributed (Jiao et al. 2019). With the continuous promotion of "the Belt and Road" initiative and the implementation of the strategy of strengthening the country through transportation, the transportation road network is expanding to the western region, which is covered with lofty mountains and steep hills. As an important part of the transportation road network, tunneling is unavoidable in the karst regions of the West. In areas with strong dissolution development, karst rock masses are subjected to dissolution, erosion, collapse, and accumulation of groundwater, resulting in the complex formation of karst rock masses. Due to the different degree of dissolution of karst rock masses, the spatial distribution, shape, and density of internal dissolution pores are directly different, which also determines the complexity of mechanical behavior, damage evolution characteristics, and failure mechanisms of karst rock masses. During tunnel construction, it is often difficult to grasp the impact of dissolution development in karst formations on the mechanical properties of karst rock masses, which affects the overall deformation and strength parameters of surrounding rock and poses a significant threat to the stability of tunnel surrounding rock (Day et al. 2004; Hamid et al. 2012; Song et al. 2012; Gutierrez et al. 2014; Li et al. 2023)

Currently, numerous scholars have conducted relevant studies on the mechanical properties of karst rock masses. In the field of experimental research, Li (2005) studied the strength and deformation characteristics of Jialing River limestone in its natural state under uniaxial and triaxial conditions and explored the mechanical properties of limestone under cyclic loading. Guo et al. (2014) carried out uniaxial compression on karst limestone specimens in natural and water-saturated states using RM-150B rock mechanics testing system, the energy features and energy mechanism in the process rock failure was studied from the perspective of energy. Chen et al. (2018) conducted experiments on karst limestone with different initial dissolution structures and water contents, revealing the effects of different initial dissolution structures and water contents on the mechanical properties and acoustic emission characteristics of karst limestone. Huang et al. (2019) took the shallow rock mass in the water level fluctuation zone of karst bank slopes in Three Gorges Reservoir area as the research object and obtained the mechanical properties of the shallow rock mass after deterioration by dissolution through field investigations as well as in-situ and laboratory tests. Wang et al. (2020) based on uniaxial compression tests with different strain rates, studied the effects of strain rate on the mechanical properties, damage modes, acoustic emission characteristics and the influence law of energy mechanism. Wang et al. (2022) used the acoustic characteristics of karst limestone under uniaxial compression tests to study the characteristics of microscopic cracks evolution as well as the rupture modes of karst limestone with different crack shapes. Due to the limited number of monitoring elements and the limitation of the monitoring instrument's own function, the above experiments are unable to obtain the full-field multivariate information of the rupture destabilization of the karst rock masses. The numerical simulation method can visualize the dynamic instability and rupture process of the dissolved rock mass, thus solving the above problems existing in indoor tests. In terms of numerical simulation research, Liu et al. (2006; 2009) studied the evolution of mechanical characteristics of karst marl at different dissolution stages by using numerical computation method. Zhu et al. (2014) constructed a numerical calculation model of karst rock mass based on the finite element numerical calculation method and investigated the relationship between the degree of dissolution and the strength of the rock mass through numerical simulation tests. Yu et al. (2018) based on the Monte Carlo method to establish a three-dimensional numerical model of random distribution of karst caves, the loading test simulation of the surrounding rock with different karst ratio and studied the influence of the weak development of karst on the strength parameters of the surrounding rock. Above

numerical simulation studies on the karst rock mass mainly used the finite element method or finite difference method, and these numerical simulation methods regard the karst rock mass as a porous continuous medium, which cannot realistically portray the process of crack initiation, propagation, and dynamic evolution leading to damage in the karst rock mass. The discrete element method has been widely promoted and applied in the field of rock mechanics and engineering in recent years due to its outstanding advantages in simulating and reproducing the fracture process of rock masses. Zhang et al. (2017) established a particle flow numerical model based on the classification of rock dissolution behavior, revealing the correlation between pore structure characteristics of karst rock masses and rock mechanics behavior, as well as the deformation and damage mechanism of rock masses. Yu et al. (2020) used image processing technology to extract dissolution features, constructed a discrete element numerical model of dissolution rock mass, and studied the microscopic deformation and failure characteristics of dissolution rock mass under uniaxial compression conditions Dong et al. (2020)via developing customized code using the Fish language, the degradation laws were coupled with UDEC to build the numerical procedure, and the ability of the proposed model to reproduce the macroscopic short- and long-term behaviors of carbonate rocks under the influence of water was validated. Zhang et al. (2021) constructed a discrete element model of dissolving reef limestone based on stochastic clustering algorithm and analyzed its deformation and failure laws and fracture evolution characteristics. Xiong et al. (2022) took the karst rock mass endowed in a place in Guizhou as the research object, used a particle flow discrete element numerical simulation method to study the damage evolution characteristics of karst fissured rock masses under uniaxial compression conditions. Although the above numerical simulation research on karst rock mass adopts discrete element numerical methods, they do not consider the influence of different dissolution degree pore structures on mechanical properties such as stress-strain relationship, compressive strength, elastic modulus, and damage characteristics of the rock mass. And there is no literature to carry out studies on the characteristics of energy evolution during the destruction of karst limestone with different degree of dissolution.

In view of this, this paper intends to use digital image processing technology to extract the pore characteristics of karst limestone and use R2V software to convert it into geometry in DWG format readable by discrete element software, to establish the particle flow discrete element numerical model of karst limestone with different degree of dissolution. Numerical simulation experiments are carried out on different degree of dissolution of karst limestone to explore the influence of different degree of dissolution on the stress-strain relationship, compressive strength and elastic modulus of limestone under uniaxial compression conditions, and to analyze the influence of the degree of dissolution on the damage characterization of limestone, such as force chain and fissure, and to reveal the mechanism of energy evolution in the destruction of limestone with different degree of dissolution under uniaxial compression conditions. The results of the study are of great significance to the stability analysis and safety control of the surrounding rocks of tunnels in karst stratum.

2. Construction of numerical model for karst limestone

2.1 Image recognition and model construction of karst limestone

The formation of karst rock masses requires two conditions simultaneously: firstly, flowing water flow with erosive capacity; secondly, rock that is soluble in water and permeable. When water collects at the surface cracks of the rock mass and penetrates the interior, the soluble substances inside will gradually dissolve, indicating the beginning of dissolution. Under the continuous erosion and infiltration of water flow, the cracks on the surface of the karst rock mass gradually develop into pore and hole structures. As the difference between the flow rate and velocity of water in the dissolution pores significantly increases, the water flow begins to concentrate and gradually increases the volume of the permeability space within the rock mass. Finally, some of the permeability space forms fissure which is larger than the size of the dissolution pores. In the later stage of pore formation, the erosion and dissolution of karst groundwater play an important role. The morphology of karst rock masses in nature is different. Therefore, their formation conditions are also different. The most basic reason for the different shapes and formation conditions of pores is the hydrodynamic conditions experienced by the pores. To study the mechanical properties and energy evolution characteristics of karst rock masses with different degree of dissolution under uniaxial compression conditions, it can be observed from field observations that the main forms of rock mass dissolution include dissolution fractures and dissolution pore types. The images of the karst rock mass are shown in Fig. 1 (Zhang et al. 2021).

The construction of the numerical model of karst limestone is mainly using digital image processing software Image J for image recognition, image binarization, denoising and secondary denoising, and then through the R2V software will be converted into DWG format files for discrete element software to read, the detailed process is shown in Fig. 2.

When using the digital image processing software Image J to process the image recognition of karst limestone, the color digital image is first converted into a gray-scale image, and then the gray-scale image is binarized. According to the differences between the dissolution cracks, pores, and fissures on the surface of the rock mass and the rock mass, the karst rock mass can be distinguished from the intact rock mass. Taking the eigenvalue (A) of the karst structure within the rock mass as the reference value, for any pixel in the digital image of the dissolution rock mass, the distance between its color value (E) and the characteristic value in the RGB color space can be calculated using equation (1)

$$H=|E-A| \tag{1}$$

Through the equation (1) if the calculated H value is less than the given pixel threshold T, the point will be automatically recognized by the software as a dissolution pore structure, and vice versa, it will be automatically recognized as a rock mass structure. The results of the digital processing of karst limestone sample taken on site are shown in Fig. 2, and the black area in Fig. 2 is the dissolution pore structure. After the extraction of the pore features of the karst rock mass, the R2V image processing software carries out the intelligent recognition of the edge of the pore structure and generates the karst rock mass specimen with the pore structure, which is then imported into the particle flow discrete element software. The construction of the discrete elemental numerical model of the karst rock is completed (Fig. 2).

2.2 Calibration of mesoscopic parameters of karst limestone

In the discrete element software PFC, the mechanical effects of karst limestone are characterized by the microscopic strength parameters between particle contacts, and the selection of microscopic parameters is the basis for the accuracy of numerical simulation experiments. Therefore, before simulation experiments, finding microscopic parameters is necessary. To obtain the microscopic parameters of karst limestone, it is necessary to obtain corresponding macroscopic mechanical parameters through indoor experiments, and continuously adjust the microscopic parameters based on the macroscopic parameters (elastic modulus, peak stress, Poisson's ratio) to minimize the error between simulation results and experimental results.

In this paper, the relatively intact karst limestone in the same place was sampled, and the RTM-150B rock mechanics test system was used to conduct uniaxial compression indoor tests on the standard cylindrical limestone specimens, and the test process and the results are shown in Fig. 3, and the corresponding macro-mechanical parameters were obtained and are listed in Table 1. According to the macro-mechanical parameters of karst limestone obtained from indoor tests, the fine-structural model of karst limestone was established, and uniaxial compression numerical simulation tests were conducted. According to the method in the literature (Geng et al. 2017) constantly adjust the microscopic strength parameters, and finally obtain the microscopic strength parameters that can fully reflect the macro-mechanical properties of the limestone, which are listed in Table 2.

The microscopic strength parameters from Table 2 were inputted into the numerical simulation experiment of uniaxial compression, and the results are shown in Fig. 4. From Fig. 4, the uniaxial compressive strength (UCS) is 91.34 MPa, the elastic modulus (E) is 42.5 GPa, and the Poisson's ratio (ν) is 0.19. The macroscopic mechanical properties are like those of the actual intact limestone under uniaxial compression experiments, which indicates that the particle flow model constructed in this paper can simulate the changes in the physical and mechanical properties of limestone before and after dissolution in a more satisfactory way.

2.3 Scheme of uniaxial compression tests by numerical simulation for karst limestone

In order to study the influence of the karst pore structure on the mechanical properties and energy evolution characteristics of karst limestone with different degree of dissolution under uniaxial compression, using the above mentioned method of karst limestone numerical modeling, based on on-site photos of rock masses with different dissolution degrees in karst areas, numerical models of karst limestone with degree of dissolution (R) of 0%, 3.28%, 6.35%, 9.86%, 12.56%, and 15.46% were constructed in PFC (Fig. 5), and the shape of the model was cylindrical with the length to diameter ratio of 2:l (100mm x50mm).

Based on the discrete element method, uniaxial compression numerical simulation experiments are carried out on the above numerical model of karst limestone with different degree of dissolution. During the numerical simulation of karst limestone, two walls are set up at the upper

and lower ends of the model specimen to simulate the upper and lower loading plates in the uniaxial compression test, and the upper and lower walls are loaded at the same rate and in opposite directions to load the numerical model. The rate of the upper and lower loading plates is controlled by the built-in fish language of the particle flow discrete element program, and the loading rate in the uniaxial compression numerical test is set to 0.5 mm/s. The axial stress, axial strain, and transverse strain of the model specimen are recorded in real time in the process of uniaxial compression discrete element numerical test of karst limestone with different degree of dissolution. After the destruction of the model specimen, the upper and lower walls stop moving, and a numerical test is finished. Repeat the above numerical test process for karst limestone with different degree of dissolution until all tests are completed.

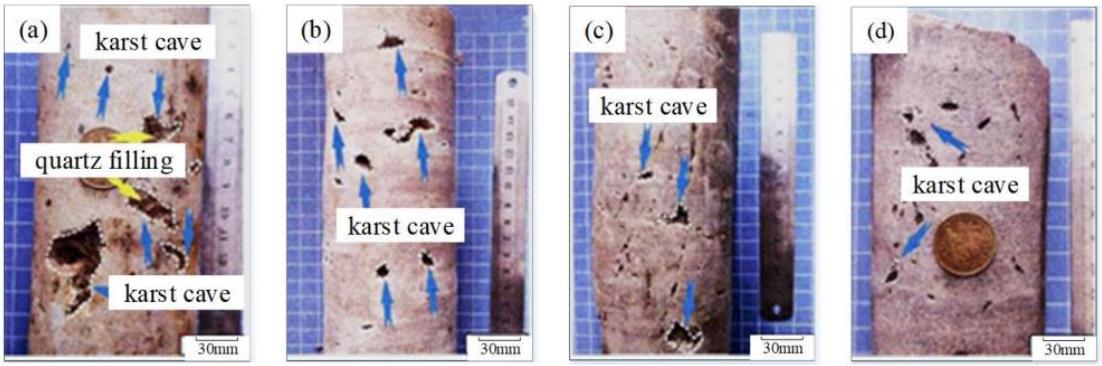

Fig. 1 Dissolution structure of karst limestone

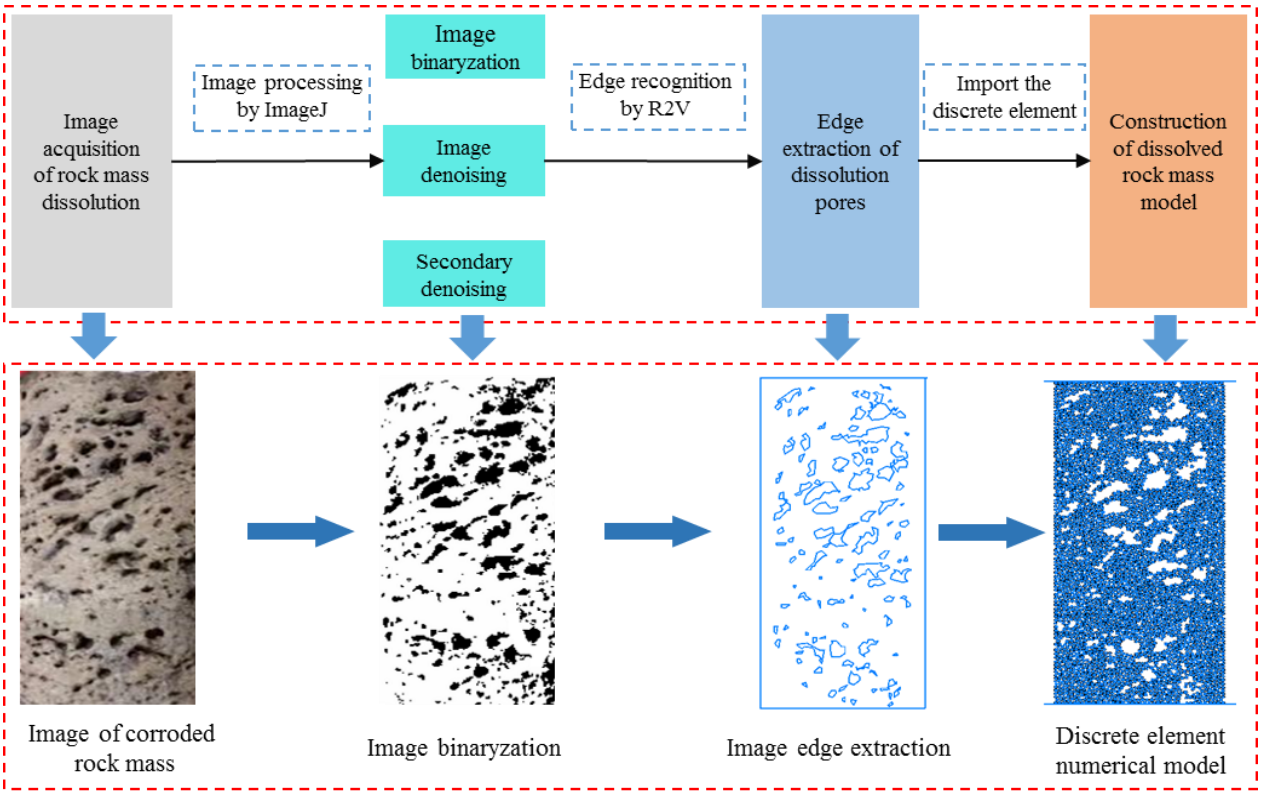

Fig. 2 Construction of numerical model for karst limestone

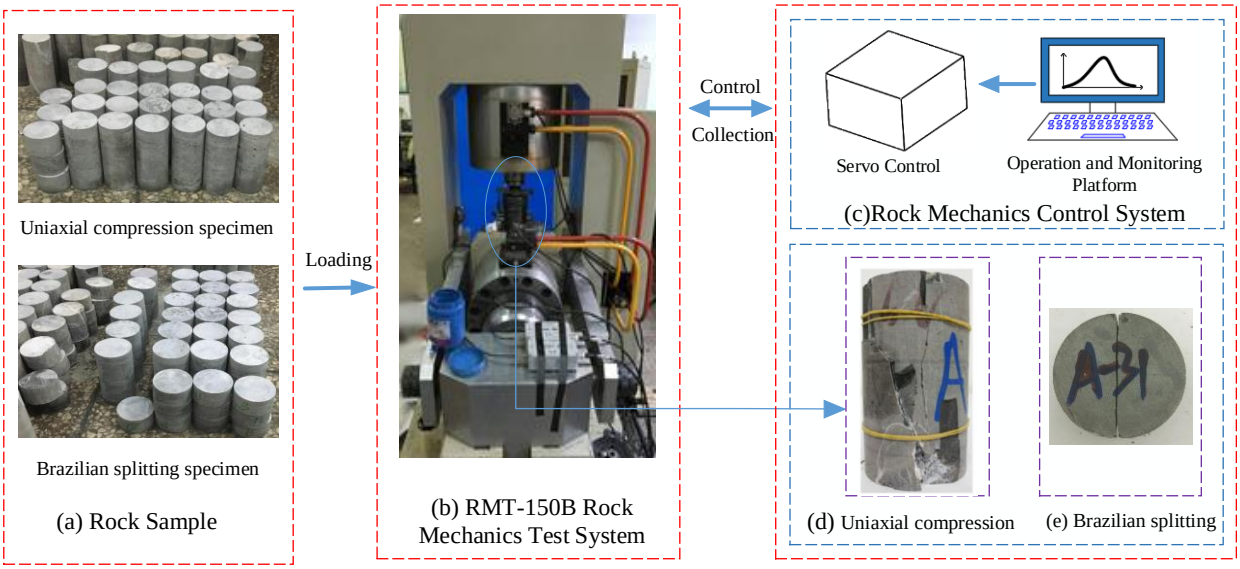

Fig. 3 Testing equipment and results

Table 1 Macroscopic mechanical parameters of limestone

Type of parameter	Rock density /g/cm^3	USC /MPa	Tensile strength /MPa	Elastic modulus /GPa	Poisson's ratio	Cohesive force /MPa	Friction angle /°
Rock materials	2.7	92	5.8	43.69	0.19	-	-
Structural plane	-	-	-	-	-	0.5	35

Table 2 Microscopic mechanical parameters of limestone

Material	Effective modulus of parallel bonding /GPa	Stiffness ratio	Linear contact effective modulus /GPa	Tangential bonding strength /MPa	Normal bonding strength /MPa	Friction angle /°	Frictional coefficient
Rock	98.6	1.5	59.2	38	7.6	70	0.70

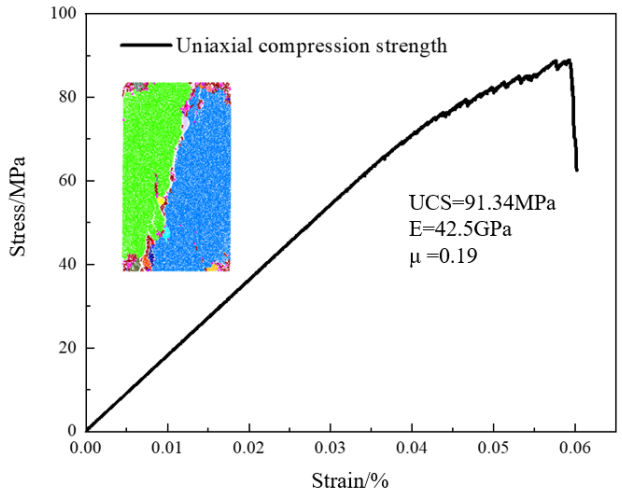

Fig. 4 Numerical test results of calibration of uniaxial compression parameters for limestone

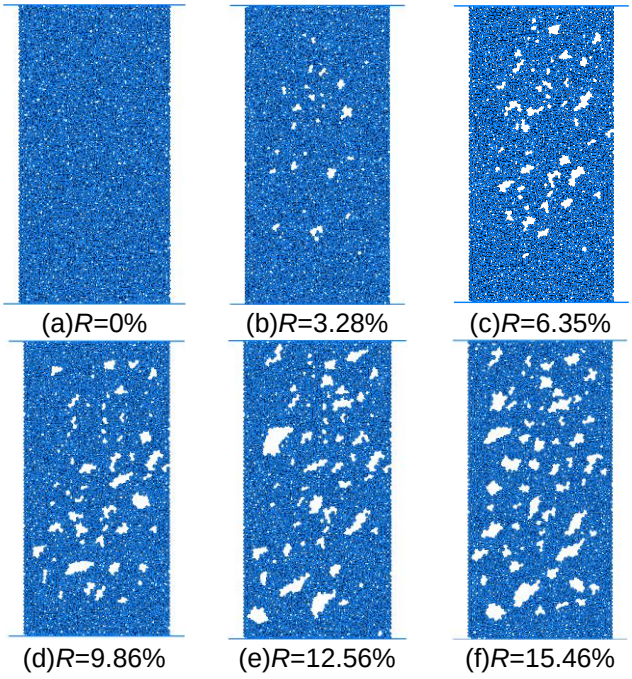

Fig. 5 Numerical calculation model for karstic limestone with different degree of dissolution

3. Mechanical properties of karst limestone with different degree of dissolution

3.1 Stress-strain relationship of karst limestone with different degree of dissolution

The stress-strain relationship of limestone with different dissolution degrees under uniaxial compression conditions is shown in Fig. 6. As shown in Fig. 6, in the uniaxial compression numerical test of karst limestone specimens, after the initial compaction, elastic deformation and plastic deformation stages of karst limestone with different degree of dissolution, the specimens gradually enter the softening stage with the continuous increase of the load. The stress-strain curves of karst limestone show obvious ductile damage characteristics, and the ductile characteristics become more and more obvious with the increase of the initial pressure. An obvious yielding platform appeared near the peak stress, and the yielding platform phenomenon was more significant when the degree of dissolution was higher.

When the karst limestone specimen is complete (e.g. R=0%) the peak of uniaxial compressive strength is relatively large, and the damage of karst limestone currently is characterized by typical brittle damage. When the dissolution degree of karst limestone reaches 3.28%, the stress-strain curve gradually slows down and the peak stress intensity decreases, with a peak intensity of 53.20 MPa (37% lower than that of the intact specimen) When the degree of dissolution reaches 6.23%, due to the gradual increase of the area and number of internal dissolution pore structure, the linear elasticity stage in the stress-strain curve of karst limestone is obviously shortened, resulting in a significant decrease in its compressive strength. When the dissolution degree of karst limestone reaches 9.86% or even higher (e.g. R=15.46%) the stress-strain curve gradually shows double-peak or multi-peak characteristics. and the higher the degree of dissolution is, the lower the value of the peak stress intensity of karst limestone is. It shows that the number and area of dissolution pores and holes in the rock mass are increasing, which makes karst limestone does not show a one-time overall damage, but more for structural damage, and the existence of pores and holes in the karst limestone destroys the structural integrity, which makes the effective bearing area in karst limestone decrease, and leads to a significant reduction in the mechanical strength of karst limestone. In addition, it can also be seen from Fig. 6 that with the increase of the degree of dissolution, the elastic phase in each stress-strain curve is gradually shortened, and the shape of the curve in the plastic deformation phase fluctuates significantly. This is because when the degree of dissolution of the rock mass increases, the combined effect of the pore structural defects and external loads intensifies, causing the stress-strain curves of karst limestone to enter plastic deformation earlier.

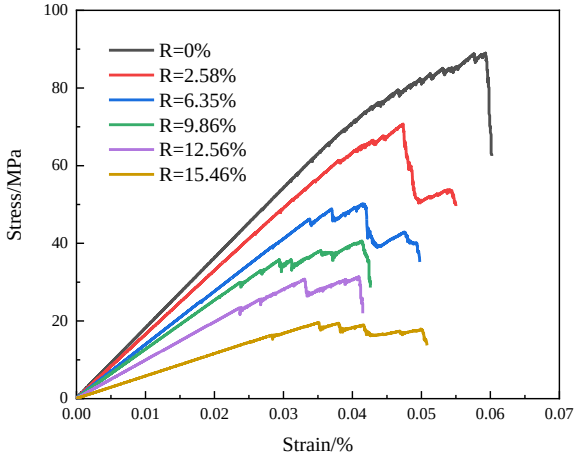

Fig. 6 Stress-strain relationship of karst limestone with different degree of dissolution

3.2 Effect of dissolution degree on uniaxial compressive strength and elastic modulus of karst limestone

According to the uniaxial compressive strength and elastic modulus of karst limestone under uniaxial compression conditions, the uniaxial compressive strength and dissolution rate R, elastic modulus and dissolution rate R were fitted with mathematical curves, and the resulting curves are shown in Fig. 7. From Fig. 7, the uniaxial compressive strength value of karst limestone gradually decreases exponentially with the increasing degree of dissolution. Moreover, when the degree of dissolution is relatively low, the decrease in uniaxial compressive strength value of karst limestone is more significant. When the dissolution degree of karst limestone is low, the decrease in its strength value slows down. The dissolution pore structure in the karst limestone mainly has a significant

impact on the mechanical properties of karst limestone during its initial formation, and as the degree of dissolution continues to increase, the decreasing trend of the mechanical strength of karst limestone becomes more significant. When the dissolution reaches a certain level, the influence of pore structure on the mechanical properties of karst limestone gradually weakens. From Fig. 8, the elastic modulus of karst limestone shows a linear decreasing trend with the increase of dissolution degree, indicating that the pore structure inside the karst limestone gradually increases during the erosion process of groundwater, resulting in linear failure of the internal structure of karst limestone.

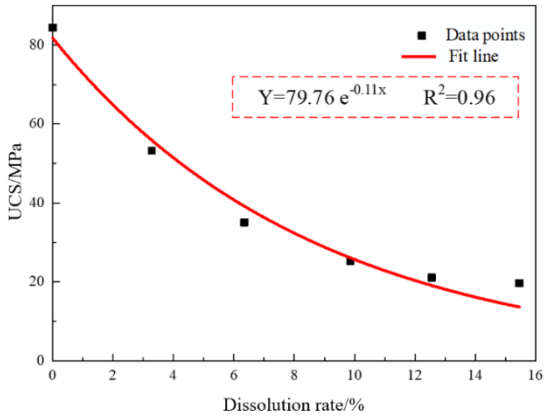

(a) Fit curve between dissolution degree and uniaxial compressive strength

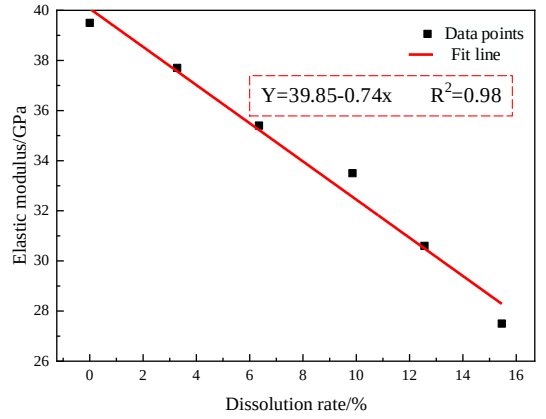

(b) Fit curve between dissolution degree and elastic modulus

Fig. 7 Fit curve between dissolution degree and mechanical parameters

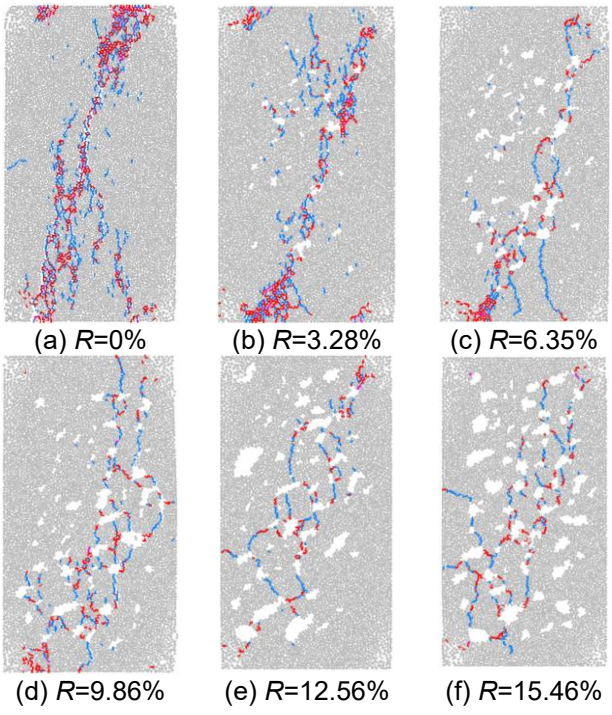

Fig. 8 Characteristics of cracks of karst limestone with different degree of dissolution at the time of failure

4. Failure characteristics of karst limestone with different degree of dissolution

4.1 Crack characteristics of karst limestone with different degree of dissolution

The final crack extension patterns of karst limestone with different degree of dissolution under uniaxial compressive loading conditions are shown in Fig. 9. In the Fig. 9, shear cracks are shown in blue and tension cracks in red. In the numerical uniaxial compression test of karst limestone, the continuous action of axial stress makes the karst limestone full of shear cracks and tension cracks at the damage surface. With the increase of the dissolution degree of karst limestone, the number of shear cracks and tension cracks is decreasing, which also reflects the decreasing uniaxial compressive strength. Under the condition of low dissolution rate, the cracks inside the karst limestone are concentrated along the direction of principal stress, and with the increase of dissolution degree, the contact degree inside the karst limestone decreases, and the distribution of cracks inside the karst limestone becomes more and more dispersed. The damage of karst limestone with higher degree of dissolution mainly occurs around the dissolution holes, so the cracks after the damage are also distributed around the dissolution holes. In addition, the cracks after the damage of karst limestone with higher degree of dissolution have certain direction, and most of the tension cracks are perpendicular to the direction of the maximum principal stress, while most of the shear cracks are in the same direction as the maximum principal stress.

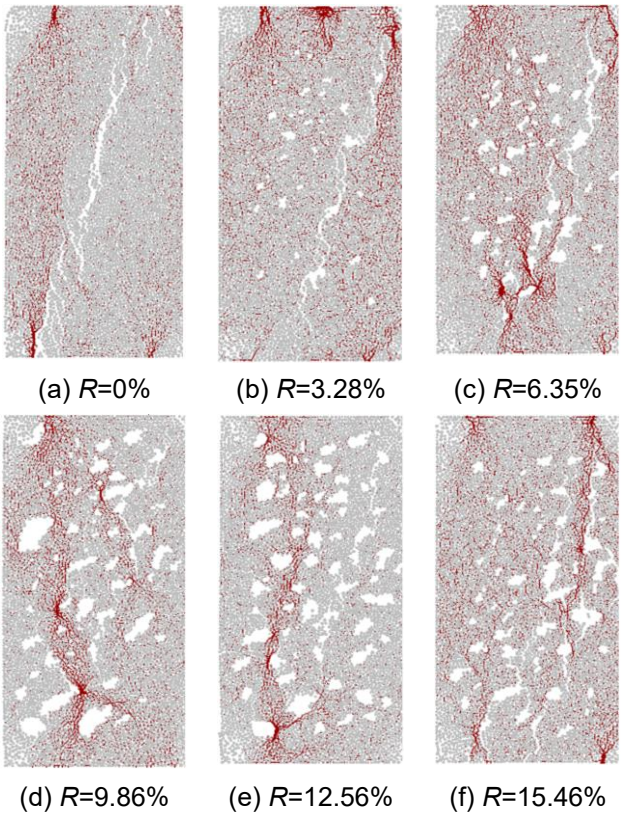

Fig. 9 Characteristics of force chains of karst limestone with different degree of dissolution at the time of failure

4.2 Force chain characteristics of karst limestone with different degree of dissolution

Fig. 10 shows the distribution of internal force chains in the karst limestone with different degree of dissolution under uniaxial compression conditions. During the loading process, to resist axial load, the internal skeleton of karst limestone will form a reasonable stress structure. After the sample is damaged, the internal contact force chain will inevitably undergo certain changes. By analyzing the distribution of the internal force chain of the sample during numerical experiment failure, the law of mutual transmission of contact forces within the karst limestone can be further explained. From Fig. 11, when the degree of dissolution is low, the stress transfer inside the corroded limestone is relatively uniform, and the entire karst limestone structure is in a stress state, which is consistent with the overall brittle failure characteristics of karst limestone revealed by the stress-strain curve. As the degree of dissolution increases, the "skeleton" effect of the limestone structure continues to weaken, and the force chains are generally dispersed. The effective structural area of karst

limestone that can bear external loads under dissolution gradually decreases, and stress concentration occurs around the pores, leading to a significant decrease in the physical and mechanical properties of karst limestone, making it prone to structural failure.

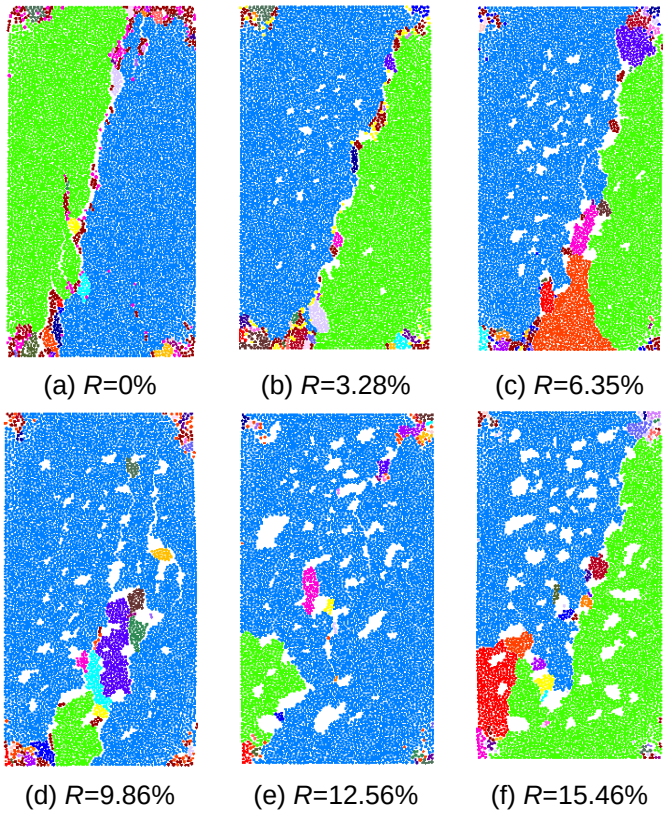

Fig. 10 Failure characteristics of karst limestone with different degree of dissolution

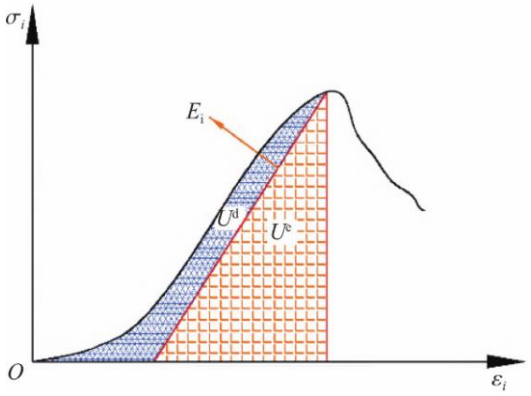

Fig. 11 Quantity relationship between U^d and U^e during rock compression process

4.3 Failure characteristics of karst limestone with different degree of dissolution

Fig. 9 shows the macroscopic mechanical damage characteristics of karst limestone different degree of dissolution under uniaxial compression loading conditions. Under uniaxial compression, the degree of dissolution has a greater influence on the damage characteristics and patterns of karst limestone specimens. When the degree of dissolution is low (e.g. R<3.28%), due to the small number of dissolution pores inside the karst limestone, the r karst limestone structure is relatively more complete. The karst limestone undergoes brittle failure under the axial load, and the surface forms a more obvious macroscopic rupture surface. When the degree of dissolution of karst limestone increases (e.g. R=6.35%), the damage to the structural surface of karst limestone specimens mainly tensile damage, and the macroscopic tensile-shear damage characteristics are formed on the structural surface. As the degree of dissolution continues to increase, the surface of karst limestone specimen no longer forms an obvious macroscopic rupture surface, and the number of fragments within the structure is also gradually reduced. This is because the presence of pore structure in the karst limestone under higher dissolution has damaged the stress skeleton in the karst limestone resulting in a significant reduction in the bearing capacity of the rock mass. Under the external loading, the karst limestone cannot form an obvious internal stress skeleton causing rapid failure of karst limestone.

5. Energy evolution characteristics of karst limestone with different degree of dissolution

5.1 Principle of Energy Calculation

The damage of the karst rock mass is the process of crack generation, expansion, and penetration, which is always accompanied by the accumulation, dissipation, and release of energy, and is the whole process of energy transfer and transformation (Ning et al. 2017; Huang et al. 2012). The uniaxial compression of the karst rock mass is often accompanied by the emergence and expansion of macroscopic cracks as well as penetration, and in the process of external loading, the strain energy accumulated in the karst rock mass is gradually released, and accordingly, the stress. strain will also change significantly. Therefore, the stress-strain curve can reflect the evolution of energy in the karst rock mass.

According to the first law of thermodynamics, it can be obtained that the work done by the machinery during the loading of the rock sample is converted into rock strain energy (Xie et al. 2005).

$$W=U=U^e+U^d \tag{2}$$

Where: U^e is the releasable elastic strain energy and U^d is the dissipated strain energy.

Fig.11 shows the relationship between the elastic strain energy U^e and the dissipative strain energy U^d during the loading damage process of the rock sample (Wang et al. 2017).

In this paper, the study is mainly carried out under uniaxial compression conditions on the karst limestone with different degree of dissolution, so that only the vertical pressure does work on the karst limestone samples, and the lateral pressure $\sigma_2=\sigma_3=0$. The expression for each strain energy within the karst limestone is:

$$U=\int_0^{\varepsilon_1}\sigma_1 d\varepsilon_1 \tag{3}$$

$$U^e=\frac{1}{2E_i}[\sigma_1^2+2\sigma_3^2-2\mu(\sigma_3^2+2\sigma_1\sigma_3)]\approx\frac{\sigma_1^2}{2E_0} \tag{4}$$

$$U^d=U-U^e \tag{5}$$

Where: "μ" is Poisson's ratio; "E" _"i" is the unloaded modulus of elasticity of rock, which can be replaced by the initial elastic modulus E_0.

5.2 Characteristics of energy evolution of karst limestone with different degree of dissolution

The internal energy evolution characteristics of karst limestone with different degree of dissolution during uniaxial compression are shown in Fig. 12. Based on the energy mechanism in the destruction process of karst limestone, the primary fissures inside the karst limestone gradually close under external load, and part of the energy absorbed within the karst limestone structure is stored in the form of elastic energy while part of it is used for the closure of the fissures as well as frictional slip of the structural surfaces. When the primary fissures have been completely closed under external loading, the karst limestone can be viewed as elastic pressure-tight body, all the energy absorbed by the karst limestone from the outside world is stored in the form of elastic energy. From Fig. 12, most of the total strain energy input is first converted into elastic strain energy, and only a small part is converted into dissipative strain energy. As the degree of dissolution increases, the total energy input to the karst limestone becomes less and less, and its stored elastic energy also becomes less and less. When the microcracks gradually sprout, but the crack development is in the "smooth" state, the energy absorbed from the outside of karst limestone is used as a small part of the internal microcrack sprouting and development, while most of the energy is still stored in the form of elastic energy. When the microcracks in the karst limestone start to expand under external loads and extend in different directions the consumption of energy increases significantly. At this time, the elastic strain energy stored in the karst limestone decreases sharply for a period and then increases slowly, while the dissipated strain energy increases sharply and then increases slowly. As the degree of dissolution increases, less energy is required form microcrack expansion. When the axial stress reaches the uniaxial compressive strength, the strain energy accumulated in the karst limestone is instantaneously released, causing macroscopic cracks to be produced on the structural surface of karst limestone and expanding through to form a more macroscopic ruptured structural surface. In the final stage, the elastic strain energy decreases sharply while the dissipated energy increases greatly, and as the deformation and damage process develops, the elastic strain energy is at a low level, and eventually the damage degree of karst limestone increases due to the large amount of energy dissipation and damage occurs due to the inability to store the remaining elastic strain energy.

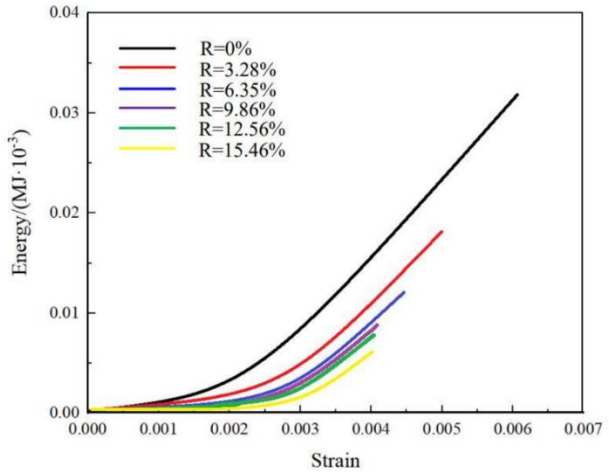

(a) The total energy U

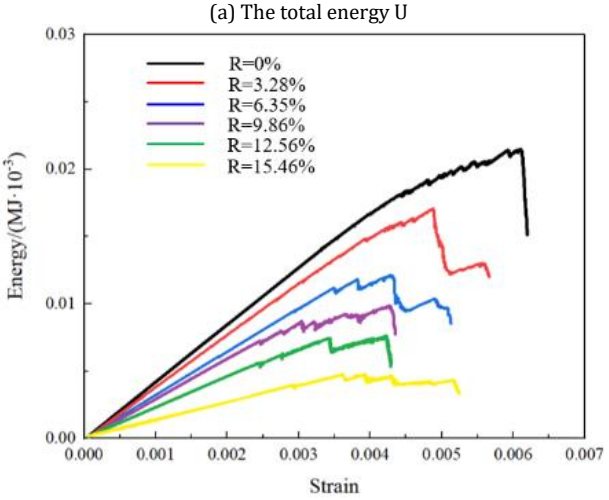

(b) The elastic strain energy U^e

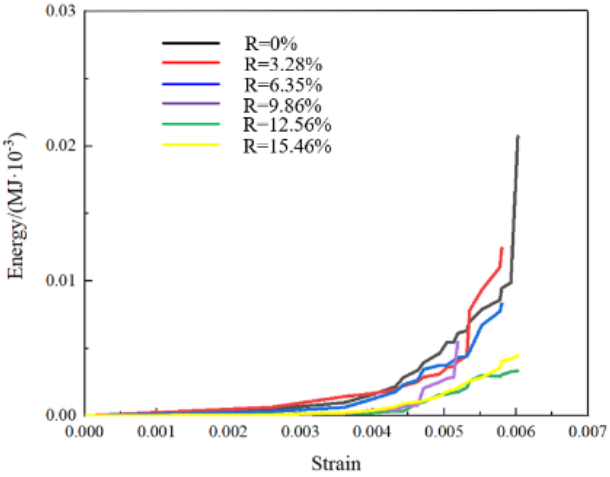

(c) The dissipative strain energy U^d

Fig. 12 Energy evolution characteristics of karst limestone with different degree of dissolution

5.3 Effect of dissolution degree on energy at peak stress under uniaxial compression condition

Fig. 13 shows the evolution of total energy U, elastic strain energy U^e, and dissipation energy U^d at the peak stress with the increase of the degree of dissolution in the karst limestone. The total energy U, elastic strain energy U^e, and dissipated strain energy U^d at the peak stress of karst limestone samples with different degree of dissolution show a decreasing trend with the increase of dissolution degree. When the dissolution degree is lower than about 3.28%, the energies at the peak stress of karst limestone samples show a faster decrease with the increase of dissolution degree; when the dissolution degree is lower than about 6.35%, the total energy U, elastic strain energy U^e of karst limestone specimen at peak stress show a still faster decrease with increasing degree of dissolution, while the dissipative strain energy U^d decreases at a slower rate; when the dissolution degree of the specimen is higher than about 6.35%, the decrease of total energy U and elastic strain energy U^e with the increase of dissolution degree is slowing down; when the dissolution degree is higher, the dissipation of energy before the peak of the specimen is more significant, the percentage of dissipated energy at the peak stress ranges from 33.75% to 41.94%, and the average is 37.85%; when the degree of dissolution is lower, the dissipated energy of karst limestone specimens at the peak stress is moderated, and the energy share ranges from 22.79% to 31.10%, with a mean value of 26.95%. The above phenomena indicate that dissolution has a significant weakening effect on the energy storage of karst limestone during compressive damage, while enhancing its energy dissipation during damage. When the karst limestone is under higher solvation conditions, the damage of karst limestone specimen continues to develop before the peak, weakening its energy storage capacity and enhancing its dissipation capacity at the peak stress.

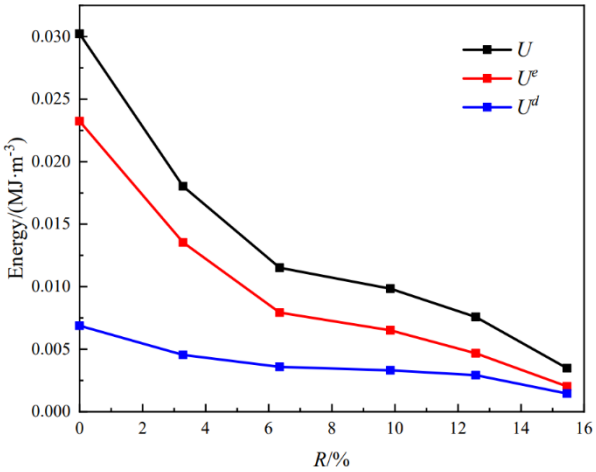

(a) Energy at peak stress

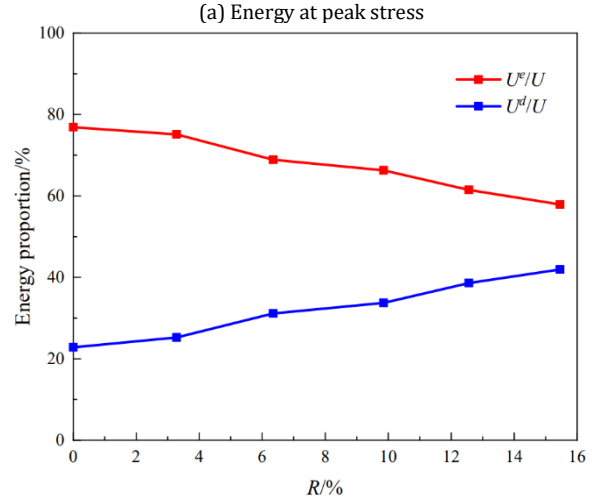

(b) Energy ratio at peak stress

Fig. 13 Energy characteristics of karst limestone with different dissolution degree at peak stress

6. Conclusions

A numerical reconstruction method for karst limestone model with different degree of dissolution based on the digital image processing technology and particle flow discrete element method was established. A series of uniaxial compression tests by discrete element numerical simulation method were conducted on karst limestone with different degree of dissolution, and the mechanical properties and energy characteristics of limestone with different degree of dissolution under uniaxial compression condition were studied. The main conclusions are as follows:

1. Numerical simulation experiments can effectively characterize the mechanical behavior of karst limestone and exhibit a similar pattern of damage to indoor experiments, indicating that the karst limestone model constructed based on digital image processing technology can effectively simulate its dissolution mechanical behavior.
2. The action of dissolution has a deteriorating effect on the mechanical properties of rock masses. The compressive strength value shows an exponential decay trend with the increase of dissolution degree, while the elastic modulus decreases linearly with the increase of dissolution degree. The higher the degree of dissolution, the more pronounced the multi peak morphology of the stress-strain curve.
3. When the degree of dissolution is low, the stress transfer inside the karst limestone is relatively uniform. When the degree of dissolution of limestone increases, the karst limestone undergoes brittle failure, forming a more obvious macroscopic fracture surface on the surface.

stress concentration occurs around the pores in the limestone sample under axial load, and the number of shear and tensile cracks is continuously decreasing. The distribution of internal force chains is dispersed, making the rock mass prone to structural failure.

4. The dissolution effect significantly weakens the energy storage limit of karst limestone samples under compression failure. During the process of karst limestone failure, most of the input total strain energy is first converted into elastic strain energy, and only a small portion is converted into dissipative strain energy. And as the degree of dissolution increases, the total energy that can be input into the eroded limestone decreases, and the elastic energy stored in it also decreases. The higher the degree of dissolution, the faster the rate of dissipation energy in karst limestone.

Acknowledgements

The authors appreciate the financial support of the National Natural Science Foundation of China (Grant No.52178388), Natural Science Foundation of Henan Province (Grant No.212300410146), China Postdoctoral Science Foundation (Grant No.2018M631114), and the Opening Project of Key Laboratory of Highway Bridge and Tunnel of Shanxi Province (Chang' University) (Grant No. 300102211517).

Conflict of interest

The authors declare that there is no conflict of interest regarding the publication of this paper.

References

Chen, J.X., Wang, Q.S., Guo, J.Q., Mechanical Properties and Acoustic Emission Characteristics of Karst Limestone under Uniaxial Compression. Adv Mater Sci Eng, 2018, pp 1–14. https://doi.org/10.1155/2018/2404256

Day, M.J., Karstic problems in the construction of Milwaukee's deep tunnels, Environ Geol, 45(6), 2004, pp 859-863. https://doi.org/10.1007/s00254-003-0945-4

Gu, D.M., Huang D., Zhang, W.G., A 2D DEM-based approach for modeling water-induced degradation of carbonate rock, International Journal of Rock Mechanics and Mining Sciences, Vol.126, 2020. https://doi.org/10.1016/j.ijrmms.2019.104188

Gutierrez, F., Parise, M., De, W.J., Jourde, H., A review on natural and human-induced geohazards and impacts in karst, Earth-Sci Rev, 138, 2014, pp 61-88.

Guo, J.Q., Liu, X.L., Qiao, C.S., Experimental study of mechanical properties and energy mechanism of karst limestone under natural and saturated states, Chinese Journal of Rock Mechanics, and Engineering, 33(02), 2014, pp 296-308.

Geng, P., Lu, Z.K., Ding, T., Research on the dynamic process simulation of rock grouting based on particle flow, Journal of railway engineering society, 34(3), 2017, pp 34-40.

Huang, D., Huang, R.Q., Zhang, Y.X., Experimental investigations on static loading rate effects on mechanical properties and energy mechanism of coarse crystal grain marble under uniaxial compression, Chinese Journal of Rock Mechanics, and Engineering, 31(2), 2012, pp 245-255.

Hamid, R.Z., Ali, U., Mostafa, S., Identifying geological hazards related to tunneling in carbonate karstic rocks-Zagros, Iran. Arabian Journal of Geosciences, 5, 2012, pp 457-464.

Huang, B.L., Yin, Y.P., Zhang, Z.H., Study on deterioration characteristics of shallow rock mass in water the level fluctuation zone of karst bank slopes in three gorges reservoir area, Chinese Journal of Rock Mechanics, and Engineering, 38(09), 2019, pp 1786-1796.

Jiao, Y.Y., Zhang, W.S., Ou, G.Z., Review of the evolution and mitigation of the water-inrush disaster in drilling-and-blasting excavated deep-buried tunnels, Hazard Control in Tunnelling and Underground Engineering, 1(1), 2019, pp 36-46.

Li, K., Pilot study on mechanics trait of tunnel karst wall rock, Southwest Jiaotong University master's degree Thesis, 2005.

Liu, H.Y., Wu, F.Q., Qi, S.W., The dissolution process, and the rock mass breakage of marlite slope in Three Gorges Reservoir Region, Coal Geology & Exploration, 34(4), 2006, pp 37-41.

Liu, H.Y., Li, Z.X., Guo, J.B., Analysis of mechanical effects of marl limestone dissolution model, Yellow River, 31(7), 2009, pp64-65.

Li, B., Zhao, C.Y., Li, J., Mechanism of mining-induced landslides in the karst mountains of Southwestern China: a case study of the Baiyan landslide in Guizhou, Landslides, 20, 2023, pp 1481–1495. https://doi.org/10.1007/s10346-023-02047-1

Ning, J.G., Wang, J., Jian, J., Estimation of crack initiation and propagation thresholds of confined brittle coal specimens based on energy dissipation theory, Rock Mechanics & Rock Engineering, (5), 2017, pp 1-16. https://doi.org/10.1007/s00603-017-1317-9

Song, K.I., Cho, G.C., Chang, S.B., Identification, remediation, and analysis of karst sinkholes in the longest railroad tunnel in South Korea, Engineering Geology, 135-136(7), 2012, pp 92-105. https://doi.org/10.1016/j.enggeo.2012.02.018

Wang, Q.S., Chen, J.X., Guo, J.Q., Acoustic emission characteristics and energy mechanism in karst limestone failure under uniaxial and triaxle compression, Bulletin of Engineering Geology & the Environment, (3), 2017, pp 1-16. https://doi.org/10.1007/s10064-017-1189-y

Wang, Q.S., Chen, J.X., Guo, J.Q., Strain rate effect on acoustic emission characteristics and energy mechanisms of karst limestone under uniaxial compression, Advances in Materials Science and Engineering, 78, 2020, pp 1427–1442. https://doi.org/10.1155/2020/6871902

Wang, G.L., Wang, R.Q., Sun, F., RA-AF characteristics of acoustic emission and failure mode of karst-fissure limestone under uniaxial compression, China Journal of Highway and Transport, 35(08), 2022, pp 118-128.

Xie, H.P., Ju, Y., Li, L.Y., Criteria for strength and structural failure of rocks based on energy dissipation and energy release principles, Chinese Journal of Rock Mechanics, and Engineering, (17), 2005, pp 3003-3010.

Xiong, S.Z., Shi, W.B., Wang, X.M., Damage and failure characteristics of karst fractured rock mass under uniaxial compression, Journal of Engineering Geology, 30(4), 2022, pp 1098 - 1110. https://doi.org/10.13544/j.cnki.jeg.2020-158

Yu, L., Li, Z., Wang, M.N., Kan, H.M., Study on the influence of weak karst development on mechanical parameters of surrounding rock, Journal of Railway Science and Engineering, 15(02), 2018, pp 435-443.

Yu, X.X., Shi, W.B., Wang, X.M., Simulation on mesoscopic deformation and failure mechanism of dissolved rock mass using digital image processing technology, Carsologica Sinica, 39(3), 2020, 409-416.

Zhang, S.R., Wang, X.H., Wang, C., Effects of pore structure and its development degree on dissolution rock mechanical characteristics, Journal of Tianjin University, 50(10), 2017, pp 1018-1028.

Zhu, L., Wang, X.Q., Nie, D.X., Stochastic method-based evaluation of corrosion rock strength parameters, Journal of Engineering Geology 22(06), 2014, pp 1034-1038. http://dx.doi.org/10.13544/j.cnki.jeg.2014.06.003

Zhang M.Z., Sun Y.F., Song Y.P., ZHAO Xiaolong, HU Guanghai. Study on the microstructure and failure characteristics of limestone in dissolution reef under uniaxial compression[J]. Chinese Journal of Computational Mechanics, 38(2), 2021, pp 222-229.